

**"Preliminary Studies Leading Toward the Development  
of a LIDAR Bathymetry Mapping Instrument"**

Dr. John M. Hill, Mr. Brendan D. Krenek, and Dr. Terry D. Kunz;  
Space Technology And Research (STAR) Center, Houston Advanced Research Center  
(HARC), The Woodlands, Texas

Mr. William Krabill and Mr. Fran Stetina;  
NASA/Goddard Space Flight Center, Greenbelt, MD

**ABSTRACT:**

The National Aeronautics and Space Administration (NASA) at Goddard Space Flight Center (GSFC) has developed a laser ranging device (LIDAR) which provides accurate and timely data of earth features. NASA/GSFC recently modified the sensor to include a scanning capability to produce LIDAR swaths. They have also integrated a Global Positioning System (GPS) and an Inertial Navigation System (INS) to accurately determine the absolute aircraft location and aircraft attitude (pitch, yaw, and roll), respectively. The sensor has been flown in research mode by NASA for many years. The LIDAR has been used in different configurations or modes to acquire such data as altimetry (topography), bathymetry (water depth), laser-induced fluorosensing (tracer dye movements, oil spills and oil thickness, chlorophyll and plant stress identification), forestry, and wetland discrimination studies.

NASA and HARC are developing a commercial version of the instrument for topographic mapping applications. The next phase of the commercialization project will be to investigate other applications such as wetlands mapping and coastal bathymetry. In this paper we report on preliminary laboratory measurements to determine the feasibility of making accurate depth measurements in relatively shallow water (approximately 2 to 6 feet deep) using a LIDAR system. The LIDAR bathymetry measurements are relatively simple in theory. The water depth is determined by measuring the time interval between the water surface reflection and the bottom surface reflection signals. Depth is then calculated by dividing by the index of refraction of water. However, the measurements are somewhat complicated due to the convolution of the water surface return signal with the bottom surface return signal. Therefore in addition to the laboratory experiments, computer simulations of the data were made to show these convolution effects in the return pulse waveform due to: a) water depth, and b) changes in bottom surface reflectivity.

**Biographical Information**

- J. Hill:** Jack Hill is the Head of the Remote Sensing/Geographic Information Systems (RS/GIS) Laboratory at the Houston Advanced Research Center (HARC). He is the Principal Investigator at HARC on the NASA LIDAR Commercialization Program.
- B. Krenek:** Brendan Krenek is a Laser Systems Specialist at HARC where he assists in laboratory feasibility demonstration experiments and system prototyping.
- T. Kunz:** Terry Kunz is Head of Laser Applications in the Space Technology And Research (STAR) Center at HARC. He is the Principal Scientist on the NASA LIDAR Commercialization Program.
- W. Krabill:** Bill Krabill is the Project Scientist for the NASA LIDAR Commercialization Project and is responsible for mission planning, instrument development, data analysis, and data interpretation. He is stationed at NASA Wallops Space Flight Center.
- F. Stetina:** Fran Stetina, stationed at the International Data Systems Office, Goddard Space Flight Center, is the Project Manager for NASA's LIDAR Commercialization Program.

## PRELIMINARY STUDIES LEADING TOWARD THE DEVELOPMENT OF A LIDAR BATHYMETRY MAPPING INSTRUMENT

### 1.0 INTRODUCTION

The National Aeronautics and Space Administration (NASA) at Goddard Space Flight Center (GSFC) has developed a laser ranging device (LIDAR) which provides accurate and timely data of earth features. NASA/GSFC recently modified the sensor to include a scanning capability to produce LIDAR swaths. They have also integrated a Global Positioning System (GPS) and an Inertial Navigation System (INS) to accurately determine the absolute aircraft location and aircraft attitude (pitch, yaw, and roll), respectively. The sensor has been flown in a research mode by NASA for many years. It has been used in different configurations or modes of the LIDAR to acquire such data as altimetry (topography) [1], bathymetry [2], laser-induced fluorosensing (tracer dye movements [3], oil spills and oil thickness [4 and 5], chlorophyll and plant stress identification [6]), forestry [7], and wetland discrimination studies [8 through 11].

NASA and HARC are developing a commercial version of the instrument for topographic mapping applications. The next phase of the commercialization project will be to investigate other applications such as wetlands mapping and coastal bathymetry.

In this paper we report on preliminary laboratory measurements to determine the feasibility of making accurate depth measurements in relatively shallow water (approximately 2 to 6 feet deep) using a LIDAR system. The LIDAR bathymetry measurements are relatively simple in theory. The water depth is determined by measuring the time interval between the water surface reflection and the bottom surface reflection signals. Depth is then calculated by dividing by the index of refraction of water. However, the measurements are somewhat complicated due to the *convolution* of the water surface return signal with the bottom surface return signal. Therefore, in addition to the laboratory experiments, computer simulations of the data were made to show these convolution effects in the return pulse waveform due to: a) water depth, and b) changes in bottom surface reflectivity.

The experiment was simplified by eliminating the water column and substituting graphite plates for the top and bottom surfaces. Depth and signal return intensities were adjusted by simply moving the plates relative to each other and intercepting different amounts of the laser beam, respectively. Section 2 describes the laboratory apparatus used in these measurements. Section 3 presents the experimental results and the computer simulations. Section 4 makes general conclusions regarding the feasibility of performing LIDAR bathymetry measurements in shallow water.

## 2.0 LABORATORY LIDAR APPARATUS DESCRIPTION

These measurements were performed at HARC's Laser Applications Laboratory. Figure 1 shows the apparatus used for performing the LIDAR experiments. This apparatus consisted of a pulsed laser, telescope, fast photodiode/amplifier, and digital oscilloscope. The  $\lambda = 532$  nm output of the Nd:YAG laser (Spectra Physics, Model GCR-11-3) emitting  $E \geq 155$  mJ/pulse in a 6-7 ns pulse width was directed approximately 50 feet down the laboratory and onto two carbon plates. The top carbon plate functioned as the water surface and the bottom carbon plate served as the bottom surface. The reflected light from the top and bottom surfaces was collected by a 1" aperture telescope. A fast photodiode (Electro-Optics Technology, Model ET-2000, 200 ps rise time) and amplifier (Stanford Research Systems, Inc., Model SR440, DC-300MHz) and digital oscilloscope (LeCroy, Model 9400, 125 MHz) detected and recorded the return laser pulse waveform, respectively. Adjusting the distance between the two carbon plates simulated different water depths; moving the plates in and out of the laser beam adjusted the strength of the top and bottom surface return signals. The distances between the two plates for these experiments were 1 foot, 3 feet, and 5 feet. For each experiment, the digital scope averaged 50 waveforms before transferring the result to the plotter.

Figure 2 shows the instrumental response of the LIDAR apparatus shown in Figure 1. In this experiment, the top carbon plate was removed and the Nd:YAG laser was in *long pulse mode* (6-7 ns FWHM pulsewidth according to manufacturer's specifications). As seen in Figure 2, the LIDAR system is recording the laser FWHM as approximately 12.8 ns. This is attributed to two factors:

1. The bandwidth of the digital scope is 125 MHz; therefore, its rise time is approximately 2.8 ns (*i.e.*,  $.35/125$  MHz), and
2. The bandwidth of the amplifier is 300 MHz, corresponding to a rise time of 1.2 ns.

The Spectra Physics Nd:YAG laser can also be operated in a *short pulse mode* which reduces the temporal pulse width by approximately a factor of 3 to about 2.5 ns; this results in only a 10% loss of pulse energy. Figure 3 shows the instrumental response with the laser in the short pulse mode. After consulting with the manufacturer, the 2.5 ns specification (alignment sensitive) applies only to the base of the center peak. Therefore, in all subsequent measurements, the laser was operated in long pulse mode.

### 3.0 RESULTS

#### 3.1 EXPERIMENTAL DATA and SIMULATIONS

Figures 4, 5, and 6 show the experimental results (rough curves) when the plates were separated by 1 foot, 3 feet, and 5 feet, respectively. Also shown in these figures are simulated data (smooth curves) of each experiment. The simulations were generated by convoluting two Gaussian lineshapes, each defined by a 12.8 ns FWHM, and different line intensities (as noted in the figure captions). These simulated data were generated using a program called COCON1.BAS (described below) and are simply best fits to the experimental data as determined by eye.

#### 3.2 ADDITIONAL COMPUTER SIMULATIONS

After understanding the experimental results above, additional computer simulations were performed to reconstruct idealized bathymetry waveform data (*i.e.*, no noise due to intermediate scattering layers located between the top and bottom surfaces) predicted in 2 to 15 feet water depths. These simulations are based on the model shown in Figure 7. In this simple model, a laser pulse of intensity  $I_0$  is shot towards the water surface. At the air - water interface a portion ( $I_1$ ) of the incident beam is reflected back towards the detector based on the water index of refraction [*i.e.*,  $I_1 = I_0(n-1)^2/(n+1)^2$ ]. The rest of the laser pulse,  $I_2 (= 1-I_1)$ , is transmitted down through the water column to the bottom surface. In this process, the laser is attenuated according to the Beer-Lambert law [ $\log(I_{\text{final}}/I_{\text{incident}}) = -\alpha\ell$ , where  $\alpha$  is the attenuation coefficient and  $\ell$  is the path length] and is represented as  $I_3$ . The beam is then reflected off the bottom surface ( $R_{\text{BS}}$ ) resulting in  $I_4$ , and attenuated again travelling up the water column to the surface. A portion of  $I_5$  is again lost at the water - air interface.  $I_6$  is reflected back in the water, and  $I_7$  is transmitted back towards the detector.

As shown in Figure 7, the two most important quantities for the generating reflected waveform simulation data are  $I_1$  and  $I_7$ . Using  $n = 1.33$  as the water index of refraction at 20°C,  $I_1$  is 2% of  $I_0$ . In general,  $I_7$  can be calculated by:

$$I_7 = (10^{-\alpha\ell})^2 (I_2)^2 (R_{\text{BS}}) (I_0).$$

Using this model, two families of simulations were generated. The first simulation used a water attenuation coefficient ( $\alpha$ ) of 0.1/foot [12] and bottom surface reflectivity ( $R_{\text{BS}}$ ) of 40%. Reflected waveform data were simulated for water depths of 1.5, 3.0, 4.5, 6.0, 7.5, and 11.3 feet corresponding to 4, 8, 12, 16, 20, and 30 ns top and bottom surface peak separations, respectively (*i.e.*, the speed of light in water was taken to be 1.33 times less than in air). This family of curves is shown in Figure 8. An analogous family of curves was generated using a bottom surface reflectivity ( $R_{\text{BS}}$ ) of 10%. These data are shown in Figure 9. As noted from Reference 12, these are reasonable values for  $\alpha$  and  $R_{\text{BS}}$ . Each of the panels in Figures 8 and 9 list the water depth, separation time between the water surface and bottom surface return pulses, and the relative line intensities for the water surface return signal ( $I_{\text{nt}_1}$ ) and the bottom surface return signal ( $I_{\text{nt}_2}$ ). The data were simulated by convoluting two 6 ns FWHM Gaussian lineshapes defined by intensities

$Int_1$  and  $Int_2$ . This simple convolution software, named "COCON1", was developed and run on an IBM compatible computer and written in basic. The software will convolute any number of lines using a Lorentzian or Gaussian lineshape (defined by the lineshape FWHM). Spectral resolution can be controlled by a combination of the total number of points in the file and the wavelength range of convolution. The convoluted spectrum can be written in wavenumbers (energy) or angstroms (wavelength). The results were plotted on a HP7475A using software developed in-house and named "TRANSPLT", also written in basic.

In the simulations shown in Figure 8 ( $\alpha = 0.1/\text{foot}$  and  $R_{BS} = 40\%$ ), the bottom return pulse is *stronger* than the surface return pulse for the 3 feet (8 ns peak separation) and 4.5 feet (12 ns peak separation) water depths. At water depths deeper than approximately 5 feet, the laser will be attenuated in a sufficient length of water column so that the surface return pulse will be the larger of the signals. In contrast, in the simulations shown in Figure 9 ( $\alpha = 0.1/\text{foot}$  and  $R_{BS} = 10\%$ ), the surface return signal is always stronger than the bottom return signal.

## 4.0 CONCLUSIONS

The following conclusions are made based on the results of these experiments and computer simulations.

1. The 125 MHz digital oscilloscope (2.8 ns rise time) was not fast enough to resolve the 6 ns FWHM pulse width of the Nd:YAG laser. Therefore, the experimental data in Figures 2, 4, 5, and 6 are not in true physical agreement with the measured block separation distances.
2. The simulated data can easily be made to agree quantitatively with the experimental data.
3. Even with the slow digital oscilloscope, top and bottom surface signals corresponding to approximate water depths of 3 feet and 5 feet were clearly discernable.
4. When the water depth is of the order of 1 to 2 feet, the recorded lineshape will simply look like a single broadened line as shown in the experimental data of Figure 4, and the top panels of the simulated data in Figures 8 and 9.
5. The simulated data in Figures 8 and 9 show the effects of the water depth and bottom surface reflectivity on the return waveform. Clearly, a trade-off exists between signal strength and signal separation between the top and bottom signal reflections. In shallow water, both top and bottom return signals should be strong, but close together in time, leading to spectrum resembling a single broadened line at 2 feet depths. As the water gets deeper, the bottom surface return pulse becomes weaker due to attenuation, but is separated farther in time from the top surface return pulse.
6. A Marquardt algorithm/fitting technique [13], or similar data reduction routine(s), would be useful for deconvoluting these lineshapes in a real bathymetry application.
7. Two (2) new digital scopes will soon be available that would nicely fill the waveform recording requirements of this bathymetry application. LeCroy will soon market their 7200/7200A digital scope equipped with a 2 Gsample/sec (500 MHz analog system bandwidth, 0.7 ns rise time) for approximately \$45,000. HP will also be marketing their 54710/54720 Mainframe digital scope equipped with a 4 Gsample/sec (1.1 GHz analog system bandwidth, 0.3 ns rise time) for approximately \$40,000. Both scopes will have a SCSI-2 (small computer systems interface) port option.
8. **Future Directions** will investigate three main topics:
  - a) range biasing as a function of scan angle,
  - b) range biasing as a function of water turbidity, and
  - c) maximum depth capability of the technique.

## 5.0 REFERENCES

1. W. B. Krabill, J. G. Collins, L. E. Link, R. N. Swift, M. L. Butler, "Airborne Laser Topographic Mapping Results from Joint NASA/U. S. Army Corps Of Engineers Experiments", *Photogrammetric Engineering and Remote Sensing*, 50(6), 685 (1984).
2. F. E. Hoge, R. N. Swift, and E. B. Frederick, "Water Depth Measurement Using An Airborne Pulsed Neon Laser System", *Appl. Opt.*, 19, 871 (1980).
3. W. B. Krabill and R. N. Swift, "Airborne LIDAR Experiments at the Savannah River Plant", NASA Technical Memorandum 4007, 1987.
4. F. E. Hoge and R. N. Swift, "Experimental Feasibility of the Airborne Measurement of Absolute Oil Fluorescence Spectral Conversion Efficiency", *Appl. Opt.*, 22, 37 (1983).
5. F. E. Hoge and R. N. Swift, "Oil Thickness Measurements Using Airborne Laser-Induced Water Raman Backscatter", *Appl. Opt.*, 19(19), 3269 (1980).
6. F. E. Hoge, R. N. Swift, and J. K. Yungel, "Feasibility of Airborne Detection of Laser-Induced Fluorescence of Green Plants. 1: A Technique for the Remote Detection of Plant Stress and Species Differentiation", *Appl. Opt.*, 23, 134 (1983).
7. G. A. McClean and G. L. Martin, "Merchantable Timber Volume Estimation Using An Airborne LIDAR System", *Canadian Journal of Remote Sensing*, 12(1), 7 (1986).
8. V. Carter, "Applications of Remote Sensing to Wetlands" in G. J. Johannsen and J. L. Sanders (Eds.) Remote Sensing for Resources Management, Ankeny, Iowa, Soil Conservation Society of America, 284-300 (1982).
9. M. K. Butera, "Remote Sensing of Wetlands", *IEEE Transactions on Geoscience and Remote Sensing*, GE-23, 383 (1983).
10. J. R. Jensen, M. E. Hodgson, E. J. Christensen, H. E. Mackey, and L. Tinney, "Remote Sensing of Inland Wetlands: A Multispectral Approach", *Photogrammetric Engineering and Remote Sensing*, 52, 87 (1986).
11. J. R. Jensen, E. W. Ramsey, H. E. Mackey, E. J. Christensen, and R. R. Sharitz, "Inland Wetland Change Detection Using Aircraft MSS Data", *Photogrammetric Engineering and Remote Sensing*, 52, 521 (1987).
12. F. E. Hoge, C. Wayne Wright, William B. Krabill, Rodney R. Buntzen, Gary D. Gilbert, Robert N. Swift, James K. Yungel, and Richard E. Berry, *Applied Optics*, 27(19), 3969 (1988).
13. W. Schreiner, M. Kramer, S. Krischer, and Y. Langsam, *PC Tech. J.*, 3, 170 (1985).

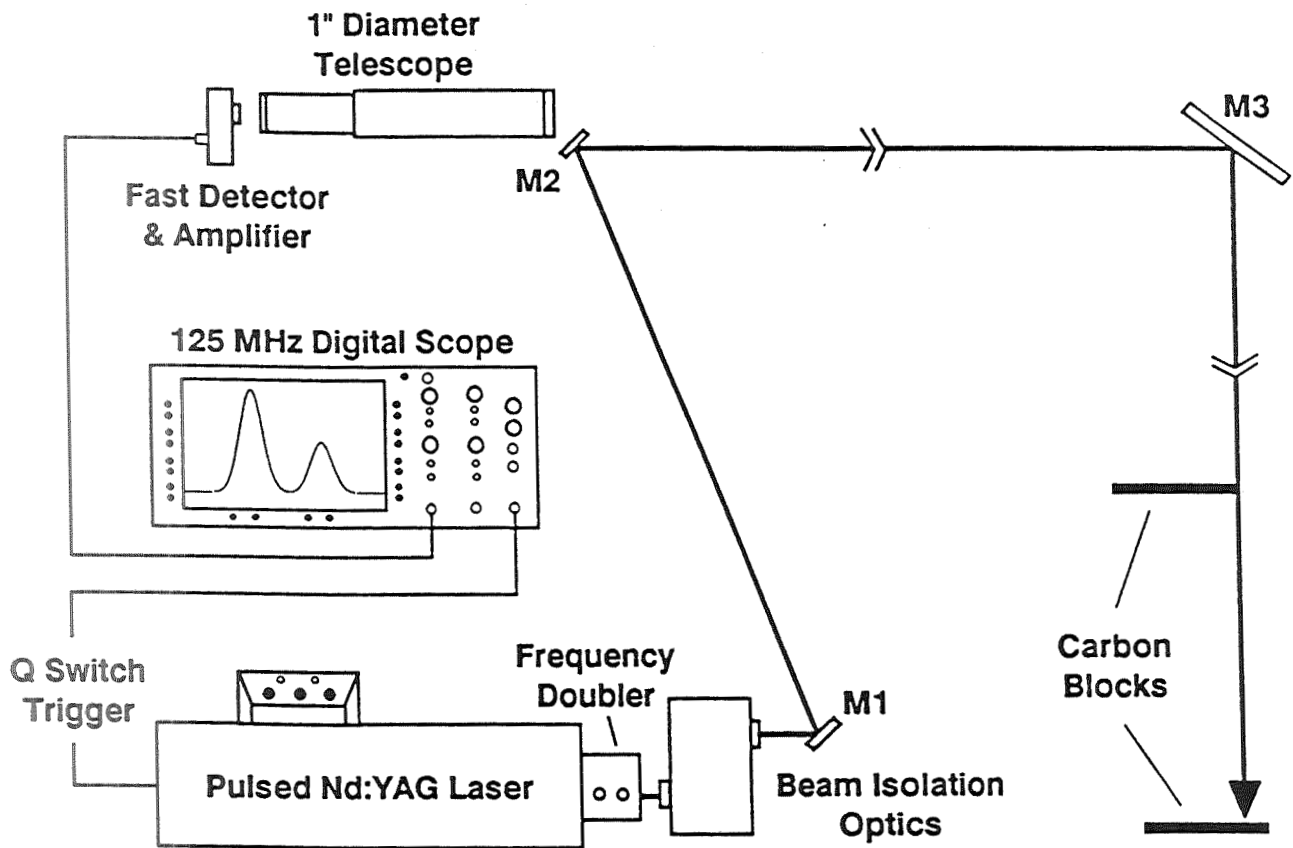


Figure 1. Laboratory LIDAR apparatus for simulating bathymetry measurements.

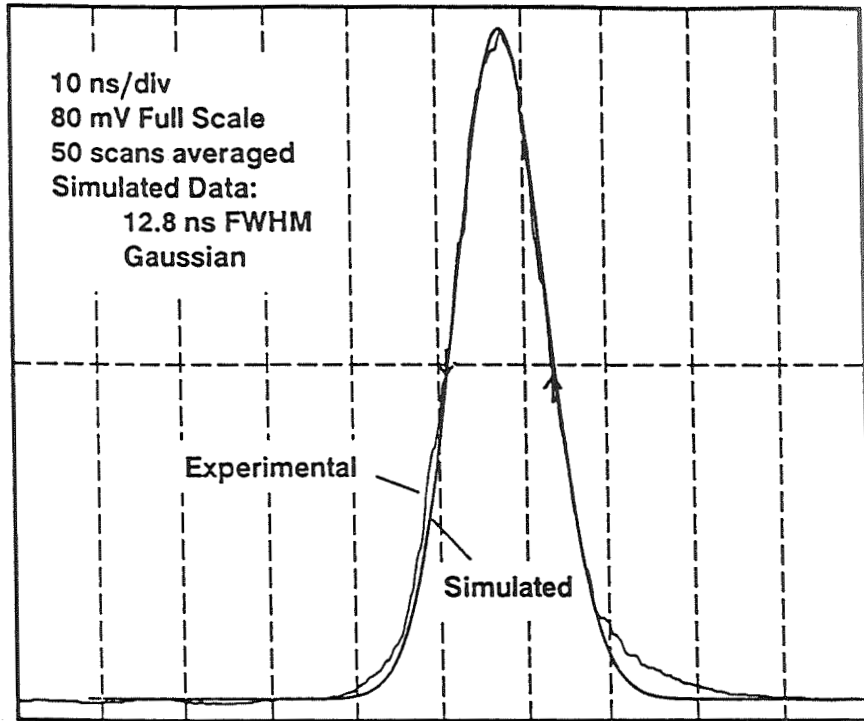


Figure 2. Instrumental response of the LIDAR apparatus shown in Figure 1 with the Nd:YAG laser in long pulse mode.

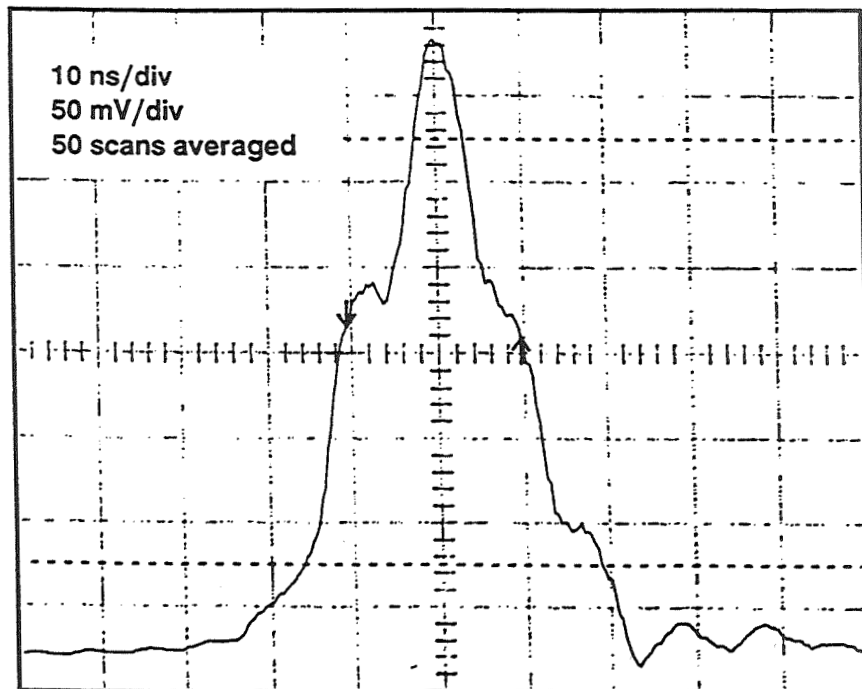


Figure 3. Instrumental response of the LIDAR apparatus shown in Figure 1 with the Nd:YAG laser in short pulse mode. Note the extra side lobes.

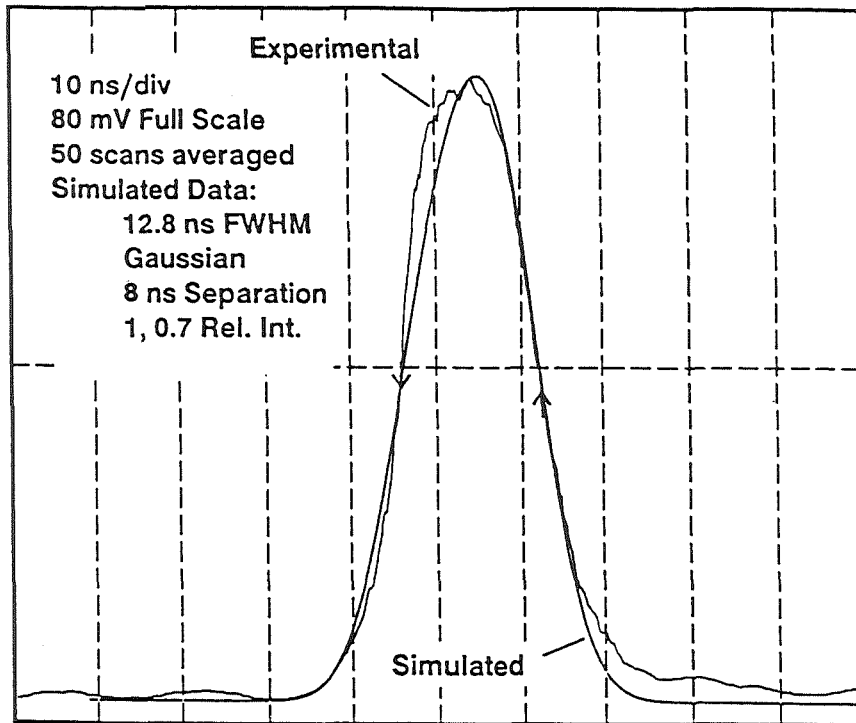


Figure 4. Experimental data (rough line) recorded with the carbon blocks spaced 1 foot apart. Simulated data (smooth line) consisting of two 12.8 ns FWHM pulses separated by 8 ns (*i.e.*, 4 feet due to *round trip travel*) with 1.0 and 0.7 relative intensities.

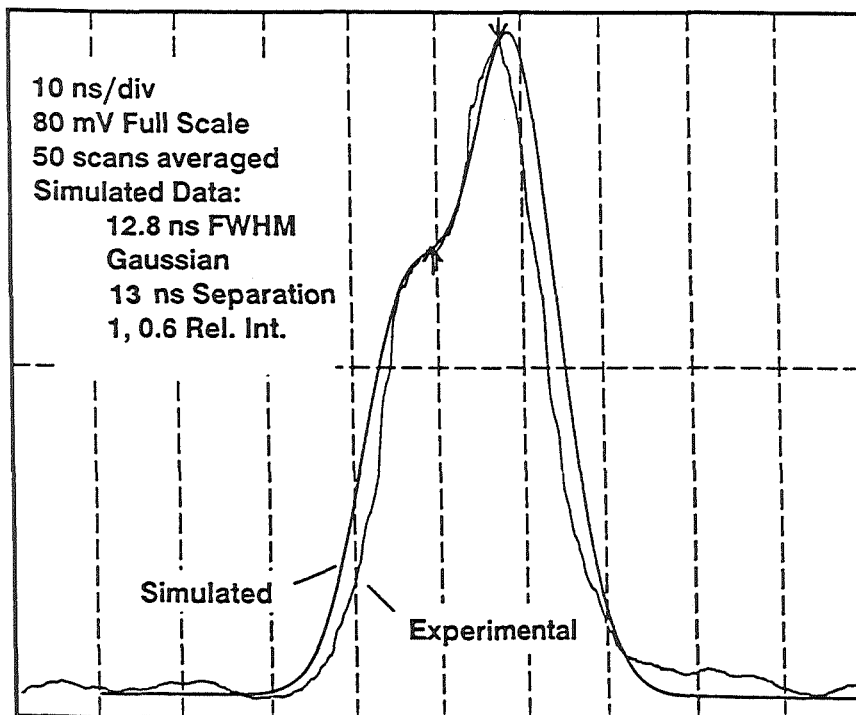


Figure 5. Experimental data (rough line) recorded with the carbon blocks spaced 3 feet apart. Simulated data (smooth line) consisting of two 12.8 ns FWHM pulses separated by 13 ns (*i.e.*, 6.5 feet *round trip travel*) with 1.0 and 0.6 relative intensities.

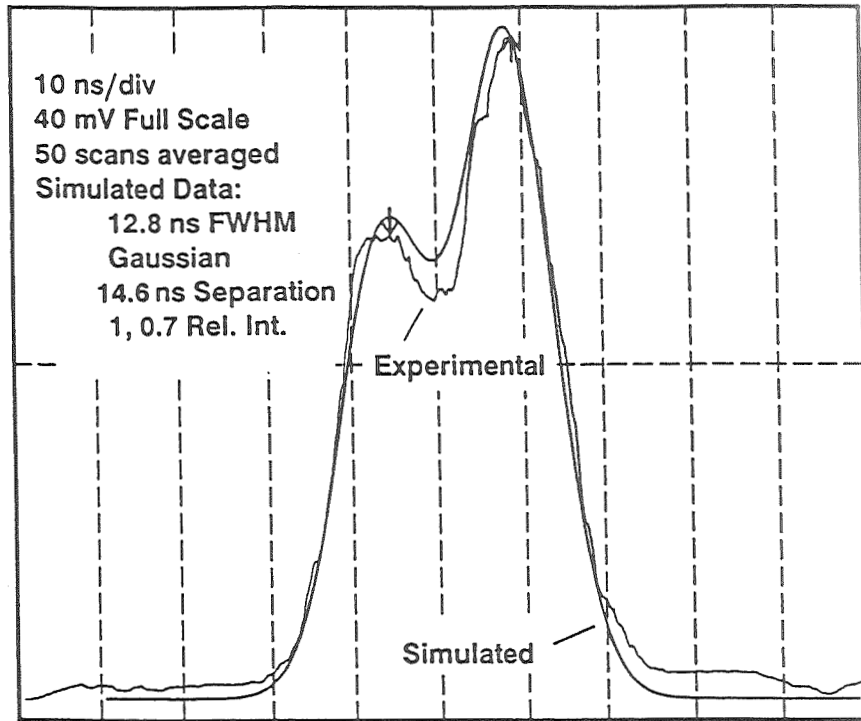


Figure 6. Experimental data (rough line) recorded with the carbon blocks spaced 5 feet apart. Simulated data (smooth line) consisting of two 12.8 ns FWHM pulses separated by 14.6 ns (*i.e.*, 7.3 feet round trip travel) with 1.0 and 0.7 relative intensities.

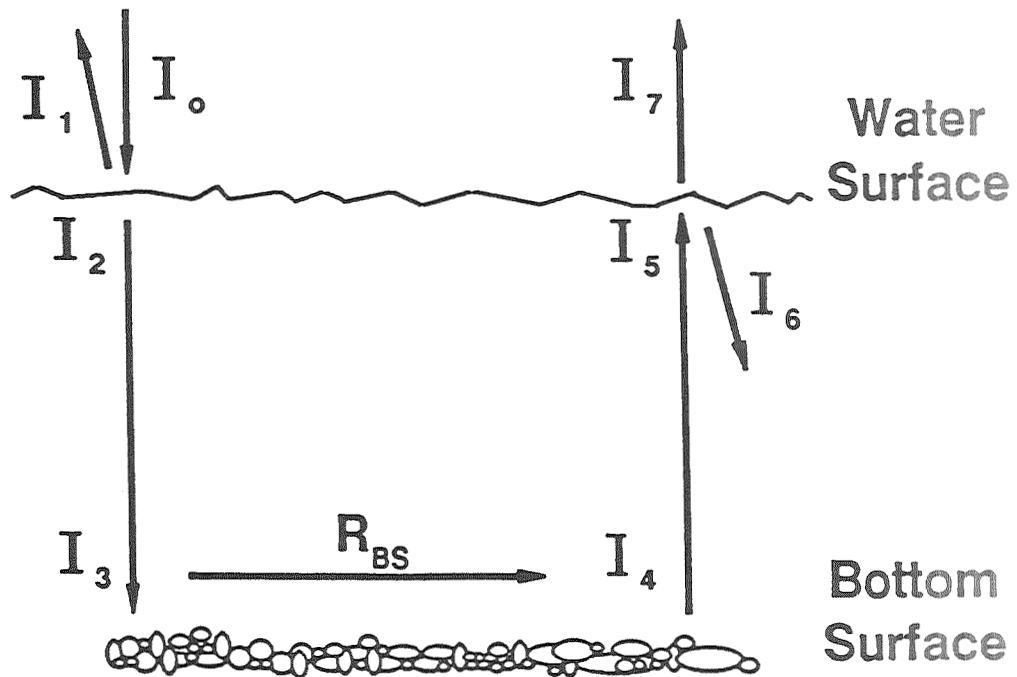


Figure 7. Simple model for determining relative return signal intensities for LIDAR bathymetry measurements.

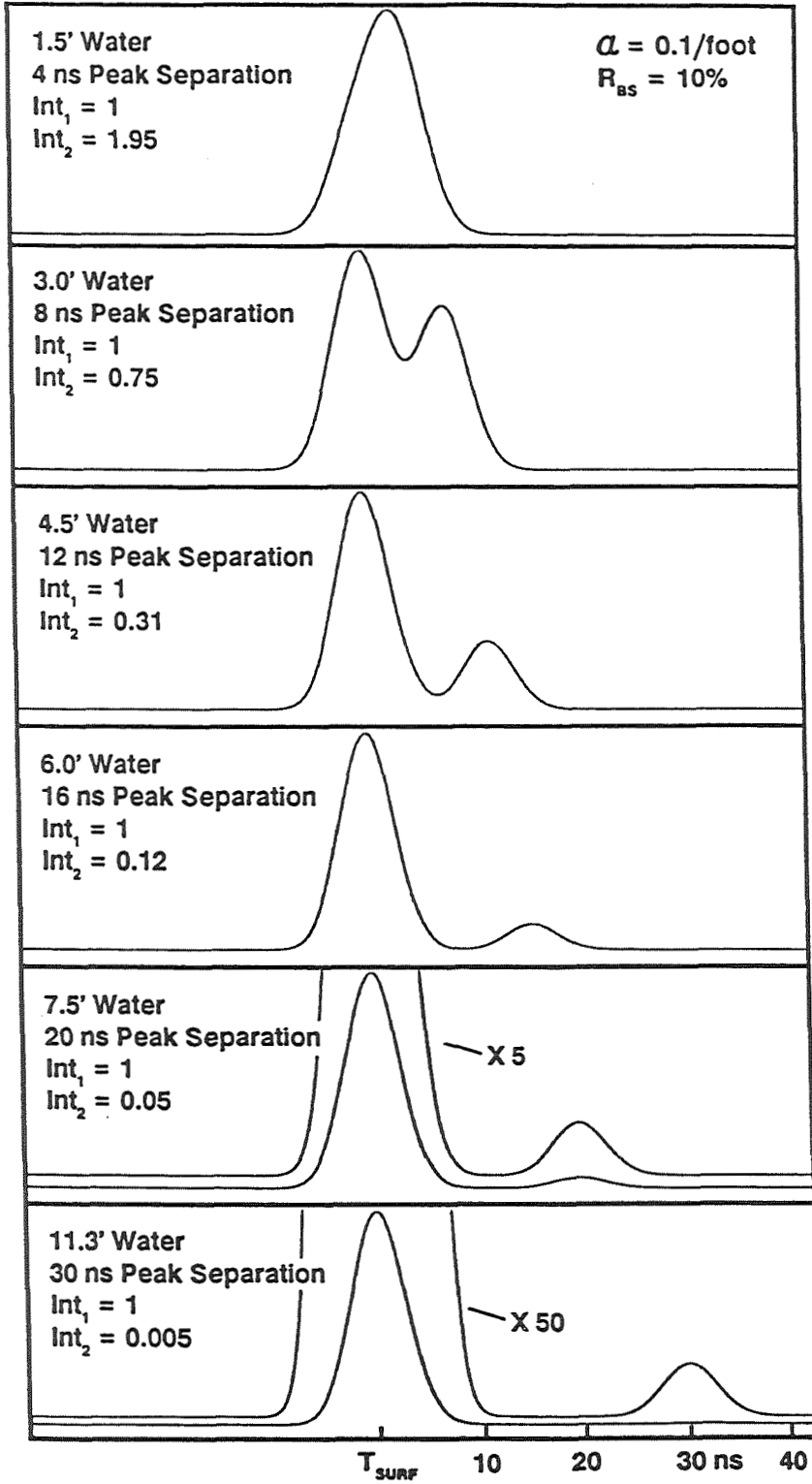


Figure 9. Family of simulated return waveform traces using a water attenuation coefficient ( $\alpha$ ) = 0.1/foot and bottom surface reflectivity ( $R_{BS}$ ) = 10%.  $T_{surf}$  designates a reference time as the peak of the water surface return pulse.